Published in final edited form as:
*Acta Biomater*. 2015 January 1; 11: 173–182. doi:10.1016/j.actbio.2014.09.011.

# Critical seeding density improves properties and translatability of self-assembling anatomically shaped knee menisci

**Pasha Hadidi**[1], **Timothy C. Yeh**[1], **Jerry C. Hu**[1], and **Kyriacos A. Athanasiou**[1,2]

[1]Department of Biomedical Engineering, University of California, Davis, One Shields Avenue, Davis, CA 95616, USA

[2]Department of Orthopedic Surgery, University of California, Davis, One Shields Avenue, Davis, CA 95616, USA

## Abstract

A recent development in the field of tissue engineering is the rise of all-biologic, scaffold-free engineered tissues. Since these biomaterials rely primarily upon cells, investigation of initial seeding densities constitutes a particularly relevant aim for tissue engineers. In this study, a scaffold-free method was used to create fibrocartilage in the shape of the rabbit knee meniscus. The objectives of this study were: (i) to determine the minimum seeding density, normalized by an area of 44 $mm^2$, necessary for the self-assembling process of fibrocartilage to occur, (ii) examine relevant biomechanical properties of engineered fibrocartilage, such as tensile and compressive stiffness and strength, and their relationship to seeding density, and (iii) identify a reduced, or optimal, number of cells needed to produce this biomaterial. It was found that a decreased initial seeding density, normalized by the area of the construct, produced superior mechanical and biochemical properties. Collagen per wet weight, glycosaminoglycans per wet weight, tensile properties, and compressive properties were all significantly greater in the 5 million cells per construct group as compared to the historical 20 million cells per construct group. Scanning electron microscopy demonstrated that a lower seeding density results in a denser tissue. Additionally, the translational potential of the self-assembling process for tissue engineering was improved though this investigation, as fewer cells may be used in the future. The results of this study underscore the potential for critical seeding densities to be investigated when researching scaffold-free engineered tissues.

### Keywords

Biomaterials; Biomechanics; Tissue engineering; Knee meniscus; Self-assembling process



Corresponding author: Kyriacos A. Athanasiou, Ph.D., P.E., Distinguished Professor of Biomedical Engineering and Orthopedic Surgery, University of California, Davis, One Shields Avenue, Davis, CA 95616, athanasiou@ucdavis.edu; Tel.: (530) 754-6645; Fax: (530) 754-5739.

## 1. Introduction

Fibrocartilage, a connective tissue found in various parts of the human body, frequently experiences degeneration, leading to conditions as diverse as osteoarthritis, difficulty eating and speaking, and back pain [1–3]. Fibrocartilaginous tissues, such as the knee meniscus, temporomandibular joint disc, and intervertebral disc, are responsible for withstanding significant mechanical loads *in vivo*, by virtue of the biochemical content of their native extracellular matrix (ECM). In particular, the collagens of the native ECM are responsible for conferring tensile strength and stiffness to these tissues, and the glycosaminoglycans (GAGs) are thought to provide compressive strength and stiffness [4, 5].

The knee meniscus represents a prime candidate for research in tissue replacement or regeneration. Meniscal lesions alone are responsible for nearly 1 million surgeries annually in the U.S. and Europe, and are the root cause of the most frequent procedures practiced by orthopedic surgeons [5, 6]. The knee meniscus displays a specific, functionally important wedge shape, as well as mechanical anisotropy between its circumferential and radial directions [7–9]. This very specific organization allows the knee meniscus to effectively transfer loading from the distal femur to the tibial plateau [10]. Thus, the biomechanical functions of the knee meniscus are inexorably tied to the structure of tissue. Importantly, the knee meniscus and all fibrocartilages display a fundamental inability to mount a healing response after structural damage is sustained due to trauma, aging, or disease, and thus represent ideal candidates for replacement by tissue engineering [10, 11].

Recently, our lab has pioneered a scaffoldless approach, termed the self-assembling process in tissue engineering, which relies upon cadherin mediated biophysical interactions that occur early during seeding of cells in a high density culture [12]. Similar studies, focused on engineering scaffold-free liver and optic tissues, have also reported all-biologic constructs displaying the presence of cadherins early during tissue culture [13, 14]. In the self-assembling process specifically, the use of a non-adherent seeding well and the upregulation of N-cadherin early during culture result in the minimization of free energy during tissue formation [15, 16]. Despite the fact that cells are not seeded within a biomaterial, the seeding well serves as a mold during this process, providing support to the developing neotissue and helping determine its final shape. This approach, first demonstrated for articular cartilage, has also been extended to the generation of fibrocartilage [17]. In particular, this has resulted in success via the creation of all-biologic constructs unhindered by intervening synthetic scaffolds [18–21]. Additionally, self-assembling constructs may lack the immunogenicity and potential toxic degradation byproducts of some biomaterial scaffolds. Finally, self-assembling constructs could avoid stress-shielding *in vivo* and have the potential for more seamless integration with native tissue [16]. However, despite these successes, additional investigations are necessary to understand and enhance structure-function relationships involving ECM content/organization, mechanical properties, and construct size and geometry.

The number of cells needed to form a construct is a non-trivial issue in tissue engineering and regenerative medicine. While one may infer that greater cell numbers may imply a larger tissue construct, this is not always the case [22, 23], and there is no guarantee that the

properties of engineered tissue constructs scale linearly as construct size increases. Furthermore, several musculoskeletal tissues, including fibrocartilage, possess relatively low cellularity. From a translational perspective, generating a tissue construct requires a large number of cells, whose acquisition from a patient or donor may or may not be feasible, especially if an investigator is employing an autologous or allogeneic approach. Interestingly, altering seeding density has repeatedly been reported to change or improve the quality of tissue constructs [24–26]. Recent work in our laboratory has demonstrated the use of this for self-assembling articular cartilage [23], although the generation of shape-specific knee meniscus fibrocartilage and the relationship of its biochemical and biomechanical properties to seeding density remain unknown.

The objectives of this study were to (i) determine the minimum seeding density, normalized by an area of 44 $mm^2$, necessary for the self-assembling process of fibrocartilage to occur, (ii) examine relevant biomechanical properties of engineered fibrocartilage, such as tensile and compressive stiffness and strength, and their relationship to seeding density, and (iii) identify a reduced, or optimal, number of cells needed to produce this biomaterial. Self-assembling fibrocartilage constructs were seeded with varying numbers of cells in the shape of the native knee meniscus using non-adherent agarose molds of constant size and cultured for four weeks. At the end of culture, construct properties were assessed. It was hypothesized that (i) a threshold seeding density existed, below which the self-assembling process would not occur, (ii) construct biomechanical and biochemical properties would increase with greater seeding densities and eventually plateau, and (iii) constructs could be seeded with fewer cells than the historical density of 20 million per construct while possessing equivalent or greater biochemical and biomechanical properties.

## 2. Materials and methods

### 2.1 Cell isolation

Bovine articular chondrocytes and meniscal cells were harvested from the legs of four 8-week-old calves (Research 87) [27, 28]. Chondrocytes were obtained from the entire surface of the distal femur, and meniscal cells were obtained from the meniscus after trimming out the outer meniscal rim. The tissues were minced into approximately 1 $mm^3$ pieces. Cartilage was digested in 0.2% (w/v) Worthington's 'collagenase type II′ enzyme mixture (Worthington) in base medium (Dulbecco's modified Eagle's medium (DMEM) (Invitrogen) with 3% (v/v) fetal bovine serum (FBS) (Benchmark), 1% (v/v) non-essential amino acids (NEAA) (Invitrogen), and 1% penicillin/streptomycin/fungizone (PSF) (Lonza) for 18 hours. Meniscal tissue was digested in a 0.25% (w/v) pronase (Sigma) in base medium for 1 hour, followed by a 0.2% (w/v) collagenase type II (Worthington) in base medium for 18 hours. After digestion, the tissues were washed and centrifuged four times using PBS and filtered through 70 μm cell strainers. Chondrocytes were frozen in DMEM with 20% (v/v) dimethylsulfoxide (DMSO) and 10% (v/v) FBS, and kept in liquid nitrogen until resuspension with freshly isolated meniscal cells for seeding, as described previously [12, 17].

### 2.2 Construct seeding and sample preparation

To generate self-assembling fibrocartilage, cells were seeded in non-adherent meniscus-shaped agarose wells formed from a rapid prototyped (ZPrinter) wedge-shaped ring mold, as described previously [29]. Meniscus-shaped ring wells were fabricated with major axis of 9.5 mm and minor axis of 7 mm, and an inner post with major axis of 4 mm and minor axis of 2.5 mm. Depth of each well was 14 mm, with an internal volume of approximately 200 μL. Approximate area of bottom surface of each meniscus shaped construct was 44 $mm^2$ [30]. Initial seeding densities were 1.25, 2.5, 5, 10, 15, and 20 million cells per construct. Each construct was seeded within 180 μL of liquid while keeping the dimensions of the well constant and varying total number of cells. To form each construct, chondrocytes and meniscal cells were seeded at a 1:1 ratio in 180 μL of a chondrogenic media formulation described previously [17]. The chondrogenic medium formulation was as follows: DMEM with GlutaMAX (Invitrogen), 100 nM dexamethasone (Sigma), 1% (v/v) PSF (Lonza), 1% (v/v) ITS+ premix (BD biosciences), 50μg/mL ascorbate-2-phosphate (Sigma), 40 μg/mL L-proline, and 100 μg/mL sodium pyruvate (Fischer Scientific). An additional 500 μL of medium was added four hours after seeding. The total volume of medium in each well was changed daily, following an internal pilot study. Media volume was 6 mL during the first week of culture and 2 mL thereafter. All cultures were kept at 37 °C with 10% (v/v) $CO_2$. After one week, tissue constructs were unconfined from their agarose wells and kept in free floating culture for an additional three weeks. During this time, constructs were cultured in a 24-well culture plate with 400 μL of agarose coated to the bottom of the well to prevent any potential adhesion of the constructs, or cells within the constructs, to the plate. After a total culture time of four weeks, construct gross morphology and wet weight were assessed before division of each construct into pieces for mechanical, biochemical, and histological analysis. Each construct was split in the same manner, with sections being taken from similar areas for each specific test. No heterogeneities were observed. All photographs of constructs for gross morphology, compressive testing, and tensile testing were taken using a Canon 100 mm f/2.8 macro lens.

### 2.3 Histology

Whole constructs were frozen at −20 °C in HistoPrep (Fisher Scientific) after culture, and additional tissue constructs were taken at days 1, 4, 7, 14, and 22 for comparison. Sections were fixed in formalin prior to staining with Safranin-O/Fast Green for GAG content and Picrosirius Red for collagen content. Other sections were fixed in acetone for immunohistochemistry (IHC) staining of collagen I and collagen II. IHC was performed with the Vectastain ABC and DAB Substrate Kits (Vector Labs) with rabbit anti-human collagen I (US Biologics) and rabbit anti-bovine collagen II antibodies (Cedar Lane Labs). The histological examination encompassed both the vertical (i.e. the full thickness) as well as the horizontal (i.e., encompassing both the major and minor axes) planes of the construct.

### 2.4 Biochemistry

Biochemical samples were weighed, lyophilized, weighed again for dry weights, and then digested in 125 μg/mL papain (Sigma) for 18 hours at 65 °C. Collagen content was quantified by a modified colorimetric hydroxyproline assay. GAG content was quantified by

a Blyscan (Biocolor) assay kit. Cell numbers were quantified by a PicoGreen dsDNA reagent (Invitrogen), using a conversion factor of 7.7 pg DNA/cell.

### 2.5 Compression testing

Uniaxial, unconfined stress-relaxation was performed on 3 mm diameter punches in order to determine compressive properties. After compressive samples were removed from constructs, each punch was photographed to determine its area using ImageJ software (NIH). Punches were taken perpendicular to the surface of constructs, after which a wedge-shaped cutting jig was used to create flat samples for compressive testing. Samples were then placed in a phosphate-buffered saline (PBS) bath on an Instron uniaxial testing machine (Model 5565, Canton, MA). Sample thickness was determined using a custom program that compressed the sample until a 0.05 N load was reached, at which point the height was recorded. The ramp rate (0.025 mm/s) and height detection load (0.05 N) were deemed appropriate for the samples tested since the load displacement curve during the height detection phase did not show overshooting of the load. Errors in measuring height during this step were estimated to occur due to slight compression of the sample. However, a back-calculation using the stiffness values of the constructs found applied strain during the height detection test to be <4%, ranging from 1.7% to 3.9%. Prior to compressive testing, samples were preconditioned at a 5% strain for 15 cycles at 1 Hz. While submerged in PBS, samples were subjected to stepwise loading at a rate of 1% $s^{-1}$ to 10% and 20% strain using a non-porous platen. Ramp duration was chosen such that the material tested would not appear more elastic than is actually the case. Specifically, ramp duration during loading was found to be similar to one-eighth of relaxation time for a viscoelastic material as suggested [31]. Following the application of 10% and 20% strains, platen position was maintained for 200 s and 450 s respectively, after which the force vs. time curve displayed negligible change, signifying the sample had relaxed. A custom program in MATLAB was used to determine the relaxation modulus and instantaneous modulus of each tested sample using a Kelvin solid model described previously [21, 32, 33] and Eq. (1) and Eq. (2) for viscoelastic materials presented below:

$$\sigma(\mathrm{t})=3/2*\mathrm{E_r}(\mathrm{u_i})/\mathrm{z}\{1+(\tau_\sigma/\tau_\mathrm{e}-1)\exp\hat{}[-(-\mathrm{t}-\mathrm{t_i})/\tau_\mathrm{e}]\} \quad (1)$$

$$\mathrm{Ei}=\mathrm{E_r}-(\tau_\sigma-\tau_\mathrm{e})\mathrm{E_r}/\tau_\mathrm{e} \quad (2)$$

Where σ(t) represents strain at time t, $E_r$ represents relaxation modulus, $E_i$ represents instantaneous modulus, $u_i$ represents strain at the start of step-wise compression, z represents tissue height, $\tau_\sigma$ and $\tau_e$ represent time constants, and $t_i$ represents the time at which peak loading occurs during stress-relaxation.

### 2.6 Tensile testing

Samples were taken in the circumferential and radial directions of the meniscus-shaped constructs, and cut into dogbone shapes to ensure failure at the desired location. A premade cutting jig was used to uniformly attain a goal gauge length of 2.3 mm and goal sample width of 0.6 mm. Tests were conducted on dogbone-shaped specimens according to ASTM

standards [34]; failure position was visually monitored during testing. Samples that did not fail at the mid-point were discarded. Grip-to-grip strain was not used, as gripping the constructs directly crushed them, yielding failure at the grips. Instead, constructs were glued to paper tabs, which were then gripped in the testing machine. All samples included in the analysis failed at the narrowest portion of the dogbone. Photographs of these samples were then used to measure the dimensions of the strained area using ImageJ. Tissue samples were adhered to strips of paper using cyanoacrylate glue, and secured to the grips of a tensile testing machine (TestResources). Samples were strained at a rate of 1% of gauge length $s^{-1}$, while displacement and load were recorded until failure of the sample at the dogbone. A relatively small strain rate was used such that the viscous contribution to tissue biomechanical properties would be relatively small, allowing for the viscoelastic samples to exhibit a linear region, as shown previously [35]. This allowed for the calculation of an equivalent Young's modulus. Data were analyzed with a custom program in MATLAB to determine the Young's modulus from the linear region of the strain curve and the ultimate tensile strength (UTS) at peak stress, as described previously [36]. Young's modulus and UTS were calculated using Eq. (3) and Eq. (4) presented below:

$$E_Y = (F/A)/(\Delta L/L) \quad (3)$$

$$UTS = F_{max}/A \quad (4)$$

Where F represents uniaxial force on the sample in the direction of testing, A represents initial cross-sectional area of the sample, ΔL represents the initial gauge length of the sample, L represents change in this gauge length, and $F_{max}$ represents the peak force attained during loading.

### 2.7 Preparation of samples for scanning electron microscopy

Construct sections for scanning electron microscopy were stored at 4° C in cacodylate buffer with 5% (w/v) sucrose after construct culture. Sections were submerged in solutions with increasing ethanol concentrations up to 100% ethanol prior to preparation for imaging. Prior to imaging, sections were critical point dried and gold sputter-coated. For each sample in a group, 8 images were taken from various locations around the tissue, with quantification measurements averaging values for all images within in a group. For density measurements, the threshold function in ImageJ was used to determine percent area of ECM versus background in an image. Percent area was then averaged over all images to calculate ECM density. A Phillips XL30 TMP scanning electron microscope was used to image samples.

### 2.8 Statistical analysis

For each biochemical and biomechanical test, n = 7 samples were used. Results were analyzed with a one-factor ANOVA followed by a Tukey's HSD post-hoc test when merited ($p < 0.05$). A two-factor ANOVA was used in tensile test results, with one factor being mechanical orientation, and the second factor being seeding density. In figures detailing results from biochemical and biomechanical assays, groups denoted without the same letter are statistically different. All data are presented as means ± standard deviations.

# 3. Results

## 3.1 Gross morphology

Constructs with seeding densities lower than 5 million cells did not form contiguous tissue that retained the form of its wedge-shaped mold when manipulated. Gross morphological images of constructs taken at the end of four weeks of culture are found in Figure 1. Thickness of constructs is shown in Table 1. Construct thickness was positively correlated with cell numbers per construct (as estimated by DNA content) as shown in Figure 1.

## 3.2 Histology

Histological sections stained for ECM biochemical content are found in Figure 2. Staining for GAG revealed a peak in Safranin-O staining at 5 million cells per construct. Similarly, Picrosirius Red staining for collagen showed a similar trend, with staining intensity greatest at 5 million cells per construct and decreasing as seeding density increased to 20 million cells per construct (historical density). All groups stained positive for collagen type I and collagen type II, as found in native meniscus fibrocartilage. Tissue from the 5 million cells per construct group maintained this trend of staining more intensely than other groups for Safranin-O and Picrosirius Red throughout various time-points (days 1, 4, 7, 14, and 22) during culture, as shown in Figure 3 and Figure 4.

## 3.3 Biochemistry

Biochemical data for collagen and GAG content were calculated per wet weight as well as per construct, as shown in Figure 5. Values from the 5 million cells per construct group were significantly greater than values from the historical 20 million cells per construct group. It is notable that seeding 5 million cells per construct resulted in significantly lower construct hydration. Increasing seeding density produced greater amounts of GAG and collagen per construct until a plateau was reached with the 10 million cells per construct group. When looking at ECM normalized to wet weight, significant differences among groups of different seeding densities were noted for both GAG and collagen production, with constructs at a seeding density of 5 million cells per construct having the highest ECM production.

## 3.4 Biomechanical properties

Results of biomechanical tests are displayed in Figure 6. Mechanical properties of the 5 million cells per construct group were significantly greater than those of the historical 20 million cells per construct group. Constructs seeded with 5 million cells per construct had the highest Young's modulus (2.4- to 11.8-fold of other seeding density groups) and UTS (2.7- to 6.7-fold of other seeding density groups) in both the circumferential and radial directions. In terms of anisotropy, constructs had higher Young's moduli and UTS in the circumferential direction than in the radial direction. Constructs seeded with 5 million cells per construct exhibited the highest instantaneous (1.5- to 2.4-fold of other seeding density groups) and relaxation (1.3- to 2.4-fold seeding density groups) moduli at both 10% and 20% strain.

### 3.5 Scanning electron microscopy

When viewed under scanning electron microscopy, construct sections displayed a network of collagen fibers. The fiber network found in constructs from the 5 million cells per construct group appeared slightly denser than the fiber network imaged at higher seeding densities. When quantified, the 5 million cells per construct group displayed a fiber density of 58% by area, as compared to 54%, 54%, and 49% for the 10, 15, and 20 million cells per construct groups, respectively.

## 4. Discussion

This study investigated the effects of varying initial seeding density in a tissue-engineered, anatomically shaped, fibrocartilaginous biomaterial. Experimental results supported the hypotheses driving this study: (i) constructs seeded with fewer than 5 million cells were not fully assayable or capable of being manipulated, and did not form contiguous engineered tissue, (ii) collagen and GAG content per construct was greater at higher initial seeding densities, and (iii) histological, biomechanical, and biochemical assays demonstrated that a lower seeding density, as normalized to initial area, was superior to the historical seeding density of 20 million cells per construct. This is the first study to report the beneficial effects of lower seeding densities in scaffold-free self-assembling fibrocartilage, and the first to show that lower seeding densities can generate biomechanically superior, anisotropic, and scaffold-free engineered knee meniscus tissue.

In assessing construct mechanical anisotropy, it was found that circumferential tensile properties were greater than radial tensile properties across all groups tested. For example, the historical 20 million cells per construct group displayed a circumferential Young's modulus 450% greater than the radial Young's modulus. Similarly, in the 5 million cells per construct group, UTS in the circumferential direction was 150% greater than UTS in the radial direction. These findings are consistent with previously published data that growth of scaffold-free tissue around a central post can result in mechanical and organizational anisotropy [29, 37]. To understand why this occurs, it is useful to imagine developing neotissue as a pre-stressed collagen network. Collagen-rich tissues engineered with fibroblasts, chondrocytes, and/or fibrochondrocytes have all been reported to contract during culture [38–40]. Since each knee meniscus construct is grown along a central post, inwards contraction is instead redirected towards contraction along this central post, resulting in anisotropic circumferential fiber alignment. Anisotropy appears to have been generated in this fashion in the engineered tissues assayed. However, a significantly dense and large enough engineered tissue must be present for this effect to occur. Thus, towards enhancing anisotropy in a clinically relevant-sized tissue, future work could examine the relationship between tissue contraction, the variation of initial seeding density, and the use of ECM modulating agents such as chondroitinase ABC or lysyl oxidase.

The data from this study suggest that a minimum threshold seeding density exists, below which the self-assembling process will not take place. This was reflected in the gross morphology of constructs seeded at lower densities, with tissue that was thin, easily compromised, and unable to maintain its shape under its own weight. These differences in construct manipulability and morphology corroborate with earlier results reporting the poor

quality of self-assembling articular cartilage constructs seeded at low densities [23]. In addition to these grossly observable differences, ECM content dropped dramatically in groups seeded with the fewest cells (1.25 and 2.5 million per construct), as compared to the best group (5 million cells per construct). The low seeding density constructs possessed less than 4% of the GAG per construct and less than 9% of the collagen per construct found in the superior 5 million cells per construct group. Additionally, final DNA content in these groups was just 3–15% of the final DNA content in the group seeded with 5 million cells. One reason for this absence of satisfactory tissue formation below a threshold seeding density may be a lack of cadherin-initiated downstream signaling. As demonstrated by earlier work, self-assembling cartilage displays high expression of N-cadherin within the first few days of culture after seeding, which allows for cell-to-cell attachment through energy minimization and tissue maturation reminiscent of native cartilage [15]. Close cell-to-cell contact mimics early stages of morphogenesis [41], and, thus, cadherin mediated downstream signaling may be crucial for satisfactory tissue formation to occur. Therefore, inadequate cell numbers below a threshold seeding density may lead to inferior construct properties partially due to a lack of cadherin-based signaling.

The results from this study increase the translational potential of self-assembling meniscus-shaped constructs. First, the results indicate that contiguous self-assembling fibrocartilage can be generated using lower seeding densities than previously demonstrated [29, 30, 42]. This overcomes a significant feasibility hurdle in the generation of a tissue-engineered meniscus, as isolation of large numbers of cells is impractical, and previous literature has reported that meniscus cells may alter their phenotype dramatically during passaging [10, 43]. Additionally, compressive properties of the tissue grown in this study, with values ranging from 100–600 kPa, are comparable to the values of compressive properties found in native meniscus [44]. Young's modulus for constructs grown in this study, lacking any growth factor treatment, reaches 3 MPa, which approaches the lower end of tensile stiffness measured for native meniscus tissue [44]. Taken together, the increased mechanical and biochemical properties, along with the lower cell number requirements, highlight the significance of growing self-assembling and other engineered tissues at appropriate initial seeding densities.

The search for a critical seeding density per initial construct area among the groups tested, resulting in tissue with the best mechanical and biochemical properties, can be viewed as a constrained minimization. Although total biochemical content per construct increased with greater initial seeding densities, tensile properties, compressive properties, and biochemical content per wet weight were greatest in engineered tissue seeded with 5 and 10 million cells per construct. A functionality index for self-assembling engineered cartilage has been described previously, and can be calculated using these parameters [20]. Whereas a result of 1 indicates that a construct possesses values equivalent to native tissue, functionality index values of 0.69, 0.52, 0.49, and 0.39 were calculated for the 5, 10, 15, and 20 million cells per construct groups, respectively. The 5 million cells per construct group displayed the greatest functionality index. Moreover, minimizing further constraints relevant to translation (e.g., construct immunogenicity, variability of construct geometry) while maintaining or increasing this functionality index represents an area for future work.

In this study, segregated fibrochondrocytes and articular chondrocytes were used in co-culture. Although the engineered tissue displayed collagen type I, collagen type II, and GAG, as found in native tissue, the constructs did not recapitulate the zonal architecture of the knee meniscus. This leads to certain limitations, as the tissue derives specific functions from the biomechanical properties and thus ECM present in each zone. In particular, the inner zone of the meniscus has relatively greater GAG content and compressive properties, while the outer zone of the tissue has relatively greater collagen type I and tensile properties [10]. These differences result from the variations in cell types in the meniscus [35]. Prior work has used multiple cell types to recapitulate these zonal variations in self-assembling meniscus tissue [36], although this study did not examine the use of different seeding densities of separate seeding densities. In the future, these techniques and others promoting cell sorting or segregation should be explored in conjunction with various seeding densities to achieve zonally variant meniscus constructs with anisotropic mechanical and biochemical properties.

The correlation of final construct dimensions with initial seeding densities also holds implications for tissue engineers to create scaffold-free tissue of controlled thickness, and/or multi-layered constructs. Importantly, this may be due to limitations in nutrient supply, especially for the groups seeded with 10, 15, or 20 million cells per construct. Future studies should continue to examine the role of varying nutrient supply and/or frequency of replenishment in scaffold-free and scaffold-based engineered tissues. Additionally, due to the relationship between final construct dimensions and initial seeding density shown in this study, tissue engineers may be precluded from generating fibrocartilage with thicknesses of several millimeters or more. However, layering strategies may be adopted in the future to bypass this limitation and/or create multilayered constructs. Tissue engineers have created multi-layered constructs, including in cartilage [45, 46], but relatively little work exists in the literature detailing all-biologic, scaffold-free constructs with multi-layered architectures. This goal is particularly relevant since the knee meniscus possesses varying ECM organization at different depths within the tissue [47, 48]. Future research could employ zonal layering with various cell types to further recapitulate native tissue-level organization. In addition, several recent studies have explored agents that enhance engineered tissue by contracting and/or cross-linking the ECM [28, 49, 50], and these should be investigated further to increase ECM organization and integrate multi-layered tissue constructs seeded at various densities.

## Conclusions

This study showed that self-assembling anatomically shaped knee meniscus fibrocartilage might be grown with a lower seeding density than used previously. In addition to this, constructs demonstrated anisotropy in the circumferential versus radial directions of the meniscus. Furthermore, constructs at a critical seeding density displayed increased mechanical and biochemical properties, and superior ECM organization as visualized by SEM. This is the first study to correlate a lower seeding density per area to superior properties in self-assembling meniscus constructs, the first study to examine the ECM structure of scaffold-free, self-assembling meniscus constructs by the use of SEM, and the first study to demonstrate a threshold seeding density exists for the self-assembling process

of fibrocartilage. Future work should quantify the beneficial effects of various anabolic (e.g., TGF-β1) and catabolic (e.g., chondroitinase ABC) stimuli upon knee meniscus tissue engineered using this critical initial seeding density.

## Supplementary Material

Refer to Web version on PubMed Central for supplementary material.

## Acknowledgments

We acknowledge funding from HHMI Med into Grad Initiative 56006769 (fellowship for P.H.), NIH R01 AR047839, and NIH R01 DE019666. P.H. and K.A.A. conceived and designed the experiments in this study, P.H. and T.Y. acquired the data, P.H., T.Y., J.C.H., and K.A.A. reviewed and interpreted the data, and P.H., J.C.H., and K.A.A. wrote and edited the paper.

## References

1. Fairbank TJ. Knee joint changes after meniscectomy. The Journal of bone and joint surgery. 1948; 30B:664–70. British volume. [PubMed: 18894618]
2. Conti PC, Ferreira PM, Pegoraro LF, Conti JV, Salvador MC. A cross-sectional study of prevalence and etiology of signs and symptoms of temporomandibular disorders in high school and university students. Journal of orofacial pain. 1996; 10:254–62. [PubMed: 9161230]
3. Harris RI, Macnab I. Structural changes in the lumbar intervertebral discs; their relationship to low back pain and sciatica. The Journal of bone and joint surgery British volume. 1954; 36-B:304–22. [PubMed: 13163117]
4. Kempson GE, Muir H, Swanson SA, Freeman MA. Correlations between stiffness and the chemical constituents of cartilage on the human femoral head. Biochim Biophys Acta. 1970; 215:70–7. [PubMed: 4250263]
5. Walker PS, Erkman MJ. The role of the menisci in force transmission across the knee. Clinical orthopaedics and related research. 1975:184–92. [PubMed: 1173360]
6. Salata MJ, Gibbs AE, Sekiya JK. A systematic review of clinical outcomes in patients undergoing meniscectomy. The American journal of sports medicine. 2010; 38:1907–16. [PubMed: 20587698]
7. Fithian DC, Kelly MA, Mow VC. Material properties and structure-function relationships in the menisci. Clinical orthopaedics and related research. 1990:19–31. [PubMed: 2406069]
8. Haut Donahue TL, Hull ML, Rashid MM, Jacobs CR. The sensitivity of tibiofemoral contact pressure to the size and shape of the lateral and medial menisci. J Orthop Res. 2004; 22:807–14. [PubMed: 15183438]
9. Leslie BW, Gardner DL, McGeough JA, Moran RS. Anisotropic response of the human knee joint meniscus to unconfined compression. Proceedings of the Institution of Mechanical Engineers Part H, Journal of engineering in medicine. 2000; 214:631–5.
10. Makris EA, Hadidi P, Athanasiou KA. The knee meniscus: structure-function, pathophysiology, current repair techniques, and prospects for regeneration. Biomaterials. 2011; 32:7411–31. [PubMed: 21764438]
11. Huey DJ, Hu JC, Athanasiou KA. Unlike bone, cartilage regeneration remains elusive. Science. 2012; 338:917–21. [PubMed: 23161992]
12. Hu JC, Athanasiou KA. A self-assembling process in articular cartilage tissue engineering. Tissue Eng. 2006; 12:969–79. [PubMed: 16674308]
13. Eiraku M, Takata N, Ishibashi H, Kawada M, Sakakura E, Okuda S, et al. Self-organizing optic-cup morphogenesis in three-dimensional culture. Nature. 2011; 472:51–6. [PubMed: 21475194]
14. Fukuda J, Sakai Y, Nakazawa K. Novel hepatocyte culture system developed using microfabrication and collagen/polyethylene glycol microcontact printing. Biomaterials. 2006; 27:1061–70. [PubMed: 16111746]

15. Ofek G, Revell CM, Hu JC, Allison DD, Grande-Allen KJ, Athanasiou KA. Matrix development in self-assembly of articular cartilage. PLoS One. 2008; 3:e2795. [PubMed: 18665220]
16. Athanasiou KA, Eswaramoorthy R, Hadidi P, Hu JC. Self-Organization and the Self-Assembling Process in Tissue Engineering. Annu Rev Biomed Eng. 2013
17. Taglieber A, Hobenreich H, Carballeira JD, Mondiere RJ, Reetz MT. Alternate-site enzyme promiscuity. Angew Chem Int Ed Engl. 2007; 46:8597–600. [PubMed: 17912724]
18. Elder BD, Athanasiou KA. Synergistic and additive effects of hydrostatic pressure and growth factors on tissue formation. PLoS One. 2008; 3:e2341. [PubMed: 18523560]
19. Natoli RM, Revell CM, Athanasiou KA. Chondroitinase ABC treatment results in greater tensile properties of self-assembled tissue-engineered articular cartilage. Tissue Eng Part A. 2009; 15:3119–28. [PubMed: 19344291]
20. Responte DJ, Arzi B, Natoli RM, Hu JC, Athanasiou KA. Mechanisms underlying the synergistic enhancement of self-assembled neocartilage treated with chondroitinase-ABC and TGF-beta1. Biomaterials. 2012; 33:3187–94. [PubMed: 22284584]
21. MacBarb RF, Makris EA, Hu JC, Athanasiou KA. A chondroitinase-ABC and TGF-beta1 treatment regimen for enhancing the mechanical properties of tissue-engineered fibrocartilage. Acta Biomater. 2013; 9:4626–34. [PubMed: 23041782]
22. Grayson WL, Bhumiratana S, Cannizzaro C, Chao PH, Lennon DP, Caplan AI, et al. Effects of initial seeding density and fluid perfusion rate on formation of tissue-engineered bone. Tissue Eng Part A. 2008; 14:1809–20. [PubMed: 18620487]
23. Revell CM, Reynolds CE, Athanasiou KA. Effects of initial cell seeding in self assembly of articular cartilage. Ann Biomed Eng. 2008; 36:1441–8. [PubMed: 18574692]
24. Puetzer JL, Bonassar LJ. High density type I collagen gels for tissue engineering of whole menisci. Acta Biomater. 2013; 9:7787–95. [PubMed: 23669622]
25. Dvir-Ginzberg M, Gamlieli-Bonshtein I, Agbaria R, Cohen S. Liver tissue engineering within alginate scaffolds: effects of cell-seeding density on hepatocyte viability, morphology, and function. Tissue Eng. 2003; 9:757–66. [PubMed: 13678452]
26. Mauck RL, Wang CC, Oswald ES, Ateshian GA, Hung CT. The role of cell seeding density and nutrient supply for articular cartilage tissue engineering with deformational loading. Osteoarthritis Cartilage. 2003; 11:879–90. [PubMed: 14629964]
27. Bhardwaj N, Nguyen QT, Chen AC, Kaplan DL, Sah RL, Kundu SC. Potential of 3-D tissue constructs engineered from bovine chondrocytes/silk fibroin-chitosan for in vitro cartilage tissue engineering. Biomaterials. 2011; 32:5773–81. [PubMed: 21601277]
28. Hadidi P, Athanasiou KA. Enhancing the mechanical properties of engineered tissue through matrix remodeling via the signaling phospholipid lysophosphatidic acid. Biochem Biophys Res Commun. 2013
29. Huey DJ, Athanasiou KA. Maturational growth of self-assembled, functional menisci as a result of TGF-beta1 and enzymatic chondroitinase-ABC stimulation. Biomaterials. 2011; 32:2052–8. [PubMed: 21145584]
30. Gunja NJ, Huey DJ, James RA, Athanasiou KA. Effects of agarose mould compliance and surface roughness on self-assembled meniscus-shaped constructs. Journal of tissue engineering and regenerative medicine. 2009; 3:521–30. [PubMed: 19658151]
31. Andrews JW, Bowen J, Cheneler D. Optimised determination of viscoelastic properties using compliant measurement systems. Soft Matter. 2013; 9:5581–93.
32. Allen KD, Athanasiou KA. Viscoelastic characterization of the porcine temporomandibular joint disc under unconfined compression. J Biomech. 2006; 39:312–22. [PubMed: 16321633]
33. Kalpakci KN, Kim EJ, Athanasiou KA. Assessment of growth factor treatment on fibrochondrocyte and chondrocyte co-cultures for TMJ fibrocartilage engineering. Acta Biomater. 2011; 7:1710–8. [PubMed: 21185408]
34. ASTM Standard E111 – 04, 2010, Standard Test Method for Young's Modulus, Tangent Modulus, and Chord Modulus. ASTM International; West Conshohocken, PA: 2010. http://www.astm.org
35. Detamore MS, Athanasiou KA. Tensile properties of the porcine temporomandibular joint disc. J Biomech Eng. 2003; 125:558–65. [PubMed: 12968581]

36. Natoli RM, Skaalure S, Bijlani S, Chen KX, Hu J, Athanasiou KA. Intracellular Na(+) and Ca(2+) modulation increases the tensile properties of developing engineered articular cartilage. Arthritis Rheum. 2010; 62:1097–107. [PubMed: 20131245]
37. Aufderheide AC, Athanasiou KA. Assessment of a bovine co-culture, scaffold-free method for growing meniscus-shaped constructs. Tissue Eng. 2007; 13:2195–205. [PubMed: 17630876]
38. Zaleskas JM, Kinner B, Freyman TM, Yannas IV, Gibson LJ, Spector M. Contractile forces generated by articular chondrocytes in collagen-glycosaminoglycan matrices. Biomaterials. 2004; 25:1299–308. [PubMed: 14643604]
39. Torres DS, Freyman TM, Yannas IV, Spector M. Tendon cell contraction of collagen-GAG matrices in vitro: effect of cross-linking. Biomaterials. 2000; 21:1607–19. [PubMed: 10885733]
40. Mueller SM, Shortkroff S, Schneider TO, Breinan HA, Yannas IV, Spector M. Meniscus cells seeded in type I and type II collagen-GAG matrices in vitro. Biomaterials. 1999; 20:701–9. [PubMed: 10353653]
41. Takeichi M. Morphogenetic roles of classic cadherins. Current opinion in cell biology. 1995; 7:619–27. [PubMed: 8573335]
42. Huey DJ, Athanasiou KA. Tension-compression loading with chemical stimulation results in additive increases to functional properties of anatomic meniscal constructs. PLoS One. 2011; 6:e27857. [PubMed: 22114714]
43. Gunja NJ, Athanasiou KA. Passage and reversal effects on gene expression of bovine meniscal fibrochondrocytes. Arthritis research & therapy. 2007; 9:R93. [PubMed: 17854486]
44. Sweigart MA, Zhu CF, Burt DM, DeHoll PD, Agrawal CM, Clanton TO, et al. Intraspecies and interspecies comparison of the compressive properties of the medial meniscus. Ann Biomed Eng. 2004; 32:1569–79. [PubMed: 15636116]
45. Levingstone TJ, Matsiko A, Dickson GR, O'Brien FJ, Gleeson JP. A biomimetic multi-layered collagen-based scaffold for osteochondral repair. Acta Biomater. 2014; 10:1996–2004. [PubMed: 24418437]
46. Kim TK, Sharma B, Williams CG, Ruffner MA, Malik A, McFarland EG, et al. Experimental model for cartilage tissue engineering to regenerate the zonal organization of articular cartilage. Osteoarthritis Cartilage. 2003; 11:653–64. [PubMed: 12954236]
47. Proctor CS, Schmidt MB, Whipple RR, Kelly MA, Mow VC. Material properties of the normal medial bovine meniscus. J Orthop Res. 1989; 7:771–82. [PubMed: 2677284]
48. Rattner JB, Matyas JR, Barclay L, Holowaychuk S, Sciore P, Lo IK, et al. New understanding of the complex structure of knee menisci: implications for injury risk and repair potential for athletes. Scandinavian journal of medicine & science in sports. 2011; 21:543–53. [PubMed: 20459477]
49. Athens AA, Makris EA, Hu JC. Induced collagen cross-links enhance cartilage integration. PLoS One. 2013; 8:e60719. [PubMed: 23593295]
50. Silva SS, Motta A, Rodrigues MT, Pinheiro AF, Gomes ME, Mano JF, et al. Novel genipin-cross-linked chitosan/silk fibroin sponges for cartilage engineering strategies. Biomacromolecules. 2008; 9:2764–74. [PubMed: 18816100]


## Appendix A. Figures with essential color discrimination

Certain figures in this article, particularly Figures 2, 3, and 4, are difficult to interpret in black and white. Full color images for these figures can be found in the online version of this article.

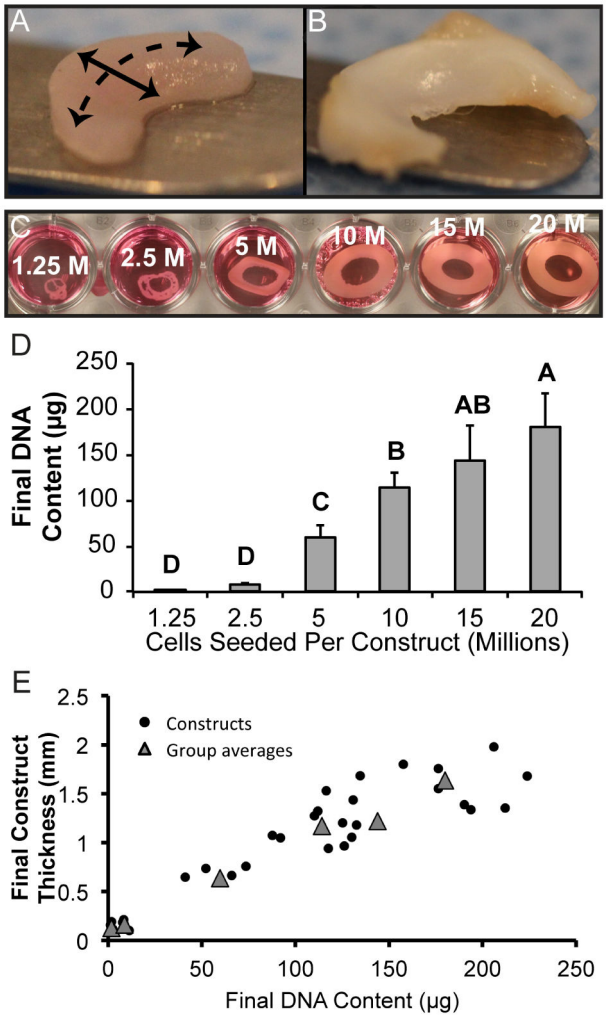


**Figure 1. Initial seeding densities and resultant morphologies of self-assembling constructs**

In general, constructs (A) maintained a wedge-shaped profile, with a circumferential direction (dashed line) and radial direction (solid line), similar to the native rabbit knee meniscus (B). Construct morphologies during culture (C) demonstrates that constructs seeded with 1.25 or 2.5 million cells per construct did not produce continuous tissue. Each construct was initially grown in a ring shape, after which it was cut in half to create the two compartments of the knee meniscus. Additionally, the 5 million cells per construct group contracted slightly during culture. 20 million cells per construct represented historical seeding density. Final DNA content of constructs (D) indicates a relationship with initial seeding density. Plot of construct final DNA content versus final construct thickness (E). Groups lacking a letter in common are significantly different ($p < 0.05$).

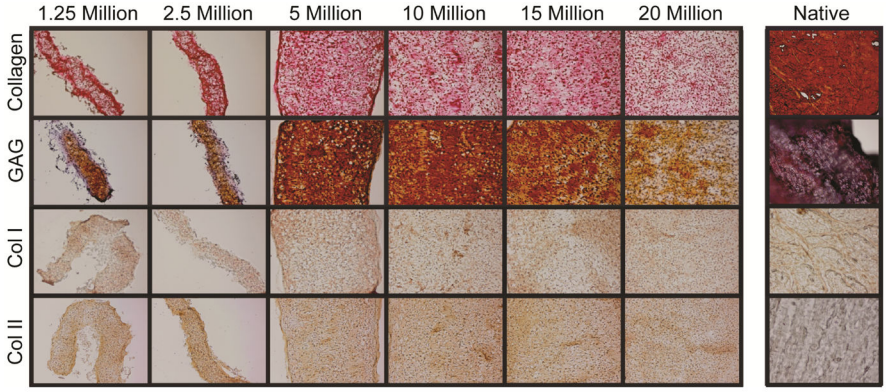


**Figure 2. Self-assembling constructs appear similar to native fibrocartilage under histological and immunohistochemical staining**

Tissue in all groups stained for collagen, GAG, and collagen types I and II, as found in native fibrocartilage. The 5 million cells per construct group displayed the most intense staining, followed by the 10 million cells per construct group. Staining became less intense in constructs seeded with more cells. Constructs seeded with 1.25 and 2.5 million cells produced thin tissues with fewer GAGS.

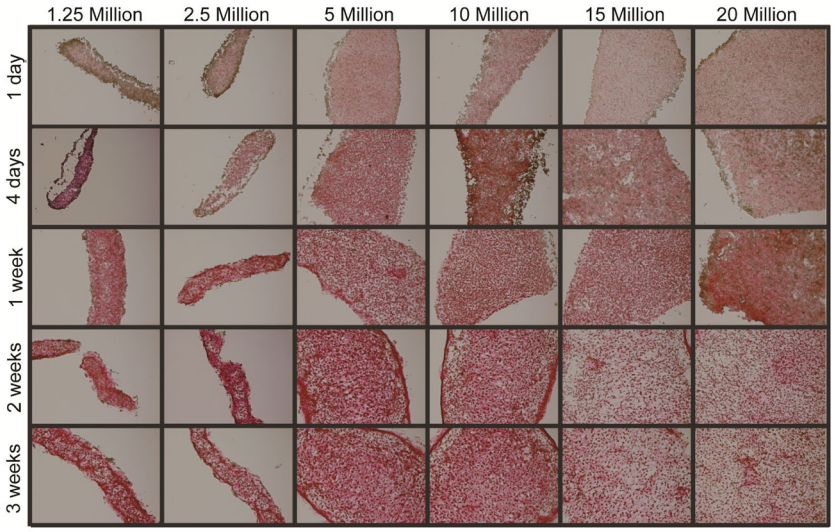


**Figure 3. Self-assembling constructs seeded with 5 or 10 million cells produce abundant collagen in culture**

Picrosirius red staining for total collagen showed increasing production over time, with the greatest amount of collagen being produced within two weeks of construct seeding. Constructs seeded with 5 or 10 million cells displayed the most collagen throughout culture. Constructs seeded with 1.25 or 2.5 million cells produced thin tissue. Constructs seeded with 15 or 20 million cells (historical seeding density) produced large tissues, which displayed relatively sparse collagen staining.

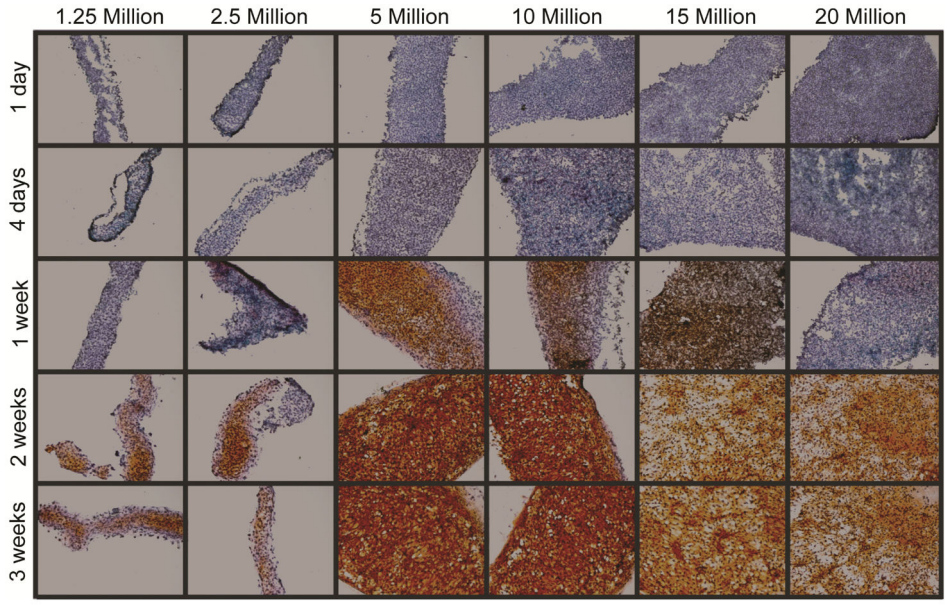


**Figure 4. Self-assembling constructs seeded with 5 or 10 million cells produce GAG more quickly in culture**

Safranin-O staining for GAG showed constructs seeded with 5 million or 10 million cells produced GAG more quickly than other groups, starting within day 7 of culture. GAG production increased over time in all groups, plateauing between day 14 and day 21 of culture. Constructs seeded with 1.25 or 2.5 million cells produced thin tissue, and GAG production began relatively later during culture. Constructs seeded with 15 or 20 million cells (historical seeding density) produced large tissues with relatively sparse GAG staining.

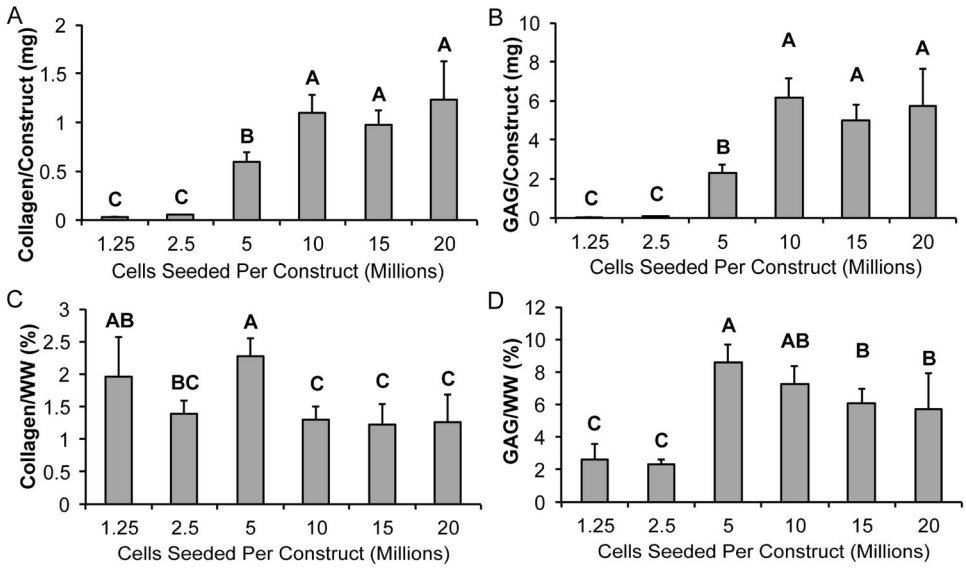


**Figure 5. Biochemical content is greater in self-assembling constructs seeded with 5 or 10 million cells**

In terms of total ECM content, total collagen per construct (A) and total GAG per construct (B) increased with greater initial seeding densities until a plateau was reached at 10 million cells per construct. When normalized to wet weight, ECM content was greatest in constructs seeded with 5 or 10 million cells. Collagen per wet weight (C) was greatest in the 5 million cells per construct group, and GAG per wet weight (D) was greatest in the 5 million cells per construct group followed by the 10 million cells per construct group. Groups lacking a letter in common are significantly different ($p < 0.05$).

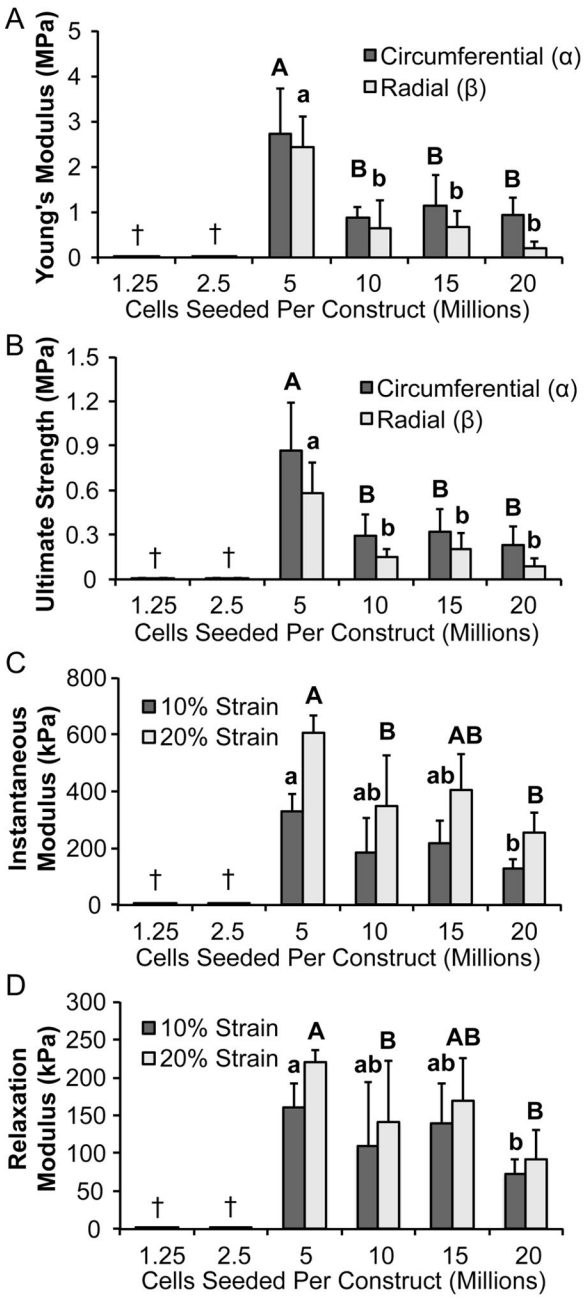


**Figure 6. Neomenisci exhibit anisotropy, and constructs seeded with 5 million cells possess greater mechanical properties**

Tensile stiffness as assessed by Young's modulus (A) was greater in both circumferential and radial directions for the 5 million cells per construct group than the historical 20 million cells per construct group. Similarly, UTS (B) was greatest in both circumferential and radial directions for the 5 million cells per construct group. Ring-shaped self-assembling constructs displayed mechanical anisotropy that recapitulated the anisotropy seen in native tissue. Across all groups, tensile properties measured in the circumferential direction of constructs were significantly greater than those measured in the radial direction (denoted by

α andβ, respectively). Furthermore, compressive stiffness as measured by instantaneous (C) was greater in the 5 million cells per construct group than other groups. Additionally, compressive stiffness as measured by relaxation modulus (D) was greater in the 5 million cells per construct group than other groups. Groups lacking a letter in common are significantly different ($p < 0.05$). Constructs seeded with fewer than 5 million cells were not assessed († = not mechanically testable).

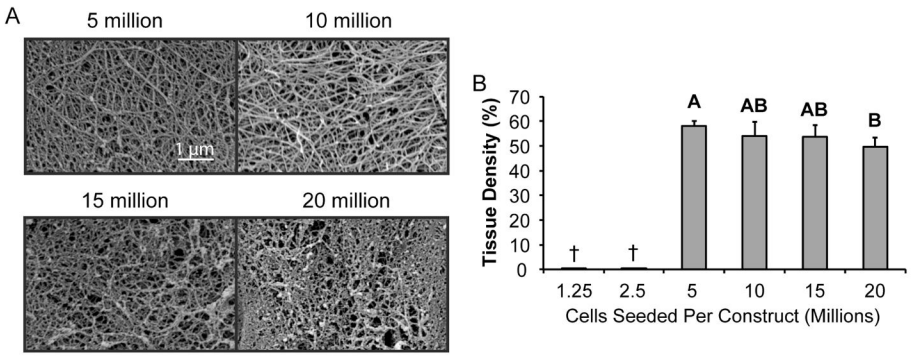


**Figure 7. Tissue density is greatest in constructs seeded with 5 million cells and decreases with higher seeding density**

When imaged with SEM, constructs seeded with 5 or 10 million cells exhibited a denser tissue with clearly defined fibers. In comparison, constructs seeded with 15 or 20 million cells displayed a less dense extracellular matrix with a less prominent collagen network. When quantified, tissue density was greatest in constructs seeded with 5 million cells, and decreased afterwards, becoming significantly less in constructs seeded at the historical density of 20 million cells per construct. Groups lacking a letter in common are significantly different ($p < 0.05$). Constructs seeded with fewer than 5 million cells were not assessed († = not imaged with SEM).

**Table 1**

Dimensions, weights, and hydrations of engineered menisci

| Group (cells seeded) | Major diameter (mm) | Minor diameter (mm) | Thickness (mm) | Weight (mg) | Hydration (%) |
|---|---|---|---|---|---|
| 1.25 million | † | † | $0.13 \pm 0.04^{D}$ | $1.79 \pm 0.40^{D}$ | $84.9 \pm 3.4^{B}$ |
| 2.5 million | $7.58 \pm 0.59^{B}$ | $4.92 \pm 0.15^{B}$ | $0.16 \pm 0.05^{D}$ | $4.04 \pm 0.54^{D}$ | $87.4 \pm 1.0^{B}$ |
| 5 million | $13.98 \pm 1.19^{A}$ | $6.18 \pm 0.71^{B}$ | $0.65 \pm 0.15^{C}$ | $26.49 \pm 3.78^{C}$ | $81.3 \pm 2.1^{A}$ |
| 10 million | $13.44 \pm 0.81^{A}$ | $9.61 \pm 1.39^{A}$ | $1.17 \pm 0.27^{B}$ | $85.15 \pm 5.61^{B}$ | $84.3 \pm 2.0^{AB}$ |
| 15 million | $13.35 \pm 0.64^{A}$ | $9.83 \pm 0.36^{A}$ | $1.22 \pm 0.31^{B}$ | $83.87 \pm 17.79^{B}$ | $86.2 \pm 1.2^{B}$ |
| 20 million | $13.62 \pm 0.36^{A}$ | $9.98 \pm 0.46^{A}$ | $1.64 \pm 0.21^{A}$ | $102.50 \pm 9.35^{A}$ | $87.5 \pm 1.4^{B}$ |

Construct morphology was quantified after culture. Diameters of constructs seeded with 2.5 million cells were less than all other groups. Thickness and construct weight increased with greater cell numbers per construct. Tissue in the 5 million cells per construct group had less water content than all other groups except the 10 million cells per construct group. Groups lacking a letter in common are significantly different ($p < 0.05$). Diameters of constructs seeded with 1.25 million cells were not assessed († = constructs diameters distorted).

*Acta Biomater*. Author manuscript; available in PMC 2016 January 01.